




## Evaluating Interaction of Cord Blood Hematopoietic Stem/Progenitor Cells with Functionally Integrated Three-Dimensional Microenvironments

SALOOMEH MOKHTARI,<sup>a†</sup> PEDRO M. BAPTISTA,<sup>b,c,d,e†</sup> DIPEN A. VYAS,<sup>a</sup> CHARLES JORDAN FREEMAN,<sup>a</sup> EMMA MORAN,<sup>a</sup> MATTHEW BROVOLD,<sup>a</sup> GUILLERMO A. LLAMAZARES,<sup>a</sup> ZANNETA LAMAR,<sup>f</sup> CHRISTOPHER D. PORADA,<sup>a</sup> SHAY SOKER,<sup>a\*</sup> GRAÇA ALMEIDA-PORADA <sup>a\*</sup>

**Key Words.** Bioengineering • Cord blood • Hematopoietic stem cells • CD34+CD38<sup>-</sup> • Liver • Pericytes • Mesenchymal stromal cells • Three-dimensional constructs • Cord blood expansion

<sup>a</sup>Wake Forest Institute for Regenerative Medicine, Winston-Salem, North Carolina, USA; <sup>b</sup>Instituto de Investigación Sanitaria de Aragón (IIS Aragón), Zaragoza, Spain; <sup>c</sup>CIBERehd, Zaragoza, Spain; <sup>d</sup>Instituto de Investigación Sanitaria de la Fundación Jiménez Díaz, Madrid, Spain; <sup>e</sup>Departamento de Bioingeniería, Universidad Carlos III de Madrid, Spain Aragon Health Sciences Institute (IACS), Zaragoza, Spain; <sup>f</sup>Hematology Oncology, Wake Forest Health Sciences, Winston-Salem, North Carolina, USA

\*Senior authors.

†Contributed equally.

Correspondence: Graça Almeida-Porada, M.D., Ph.D., Wake Forest Institute for Regenerative Medicine, 391 Technology Way, Winston-Salem, North Carolina 27157-1083, USA. Telephone: (336) 716-8672; e-mail: galmeida@wakehealth.edu; or Shay Soker, Ph.D., Wake Forest Institute for Regenerative Medicine, 391 Technology Way, Winston-Salem, North Carolina 27157-1083, USA. Telephone: (336) 716-8672; ssoker@wakehealth.edu

Received June 13, 2017; accepted for publication December 26, 2017; first published Month 00, 2018.

<http://dx.doi.org/10.1002/sctm.17-0157>

This is an open access article under the terms of the Creative Commons Attribution-NonCommercial-NoDerivs License, which permits use and distribution in any medium, provided the original work is properly cited, the use is non-commercial and no modifications or adaptations are made.

### ABSTRACT

Despite advances in *ex vivo* expansion of cord blood-derived hematopoietic stem/progenitor cells (CB-HSPC), challenges still remain regarding the ability to obtain, from a single unit, sufficient numbers of cells to treat an adolescent or adult patient. We and others have shown that CB-HSPC can be expanded *ex vivo* in two-dimensional (2D) cultures, but the absolute percentage of the more primitive stem cells decreases with time. During development, the fetal liver is the main site of HSPC expansion. Therefore, here we investigated, *in vitro*, the outcome of interactions of primitive HSPC with surrogate fetal liver environments. We compared bioengineered liver constructs made from a natural three-dimensional-liver-extracellular-matrix (3D-ECM) seeded with hepatoblasts, fetal liver-derived (LvSt), or bone marrow-derived stromal cells, to their respective 2D culture counterparts. We showed that the inclusion of cellular components within the 3D-ECM scaffolds was necessary for maintenance of HSPC viability in culture, and that irrespective of the microenvironment used, the 3D-ECM structures led to the maintenance of a more primitive subpopulation of HSPC, as determined by flow cytometry and colony forming assays. In addition, we showed that the timing and extent of expansion depends upon the biological component used, with LvSt providing the optimal balance between preservation of primitive CB HSPC and cellular differentiation. STEM CELLS TRANSLATIONAL MEDICINE 2018;7:271–282

### SIGNIFICANCE STATEMENT

During development, the fetal liver is the main site of hematopoietic stem/progenitor cell (HSPC) expansion. Herein, the authors manufactured unique constructs built upon a natural 3-D liver extracellular matrix, into which seeded fetal liver-derived stromal cells (LvSt), or hepatoblasts (HpB), become functionally integrated and assembled, and investigated the outcome of HSPC interactions with these microenvironmental-mimetic niches. Since little is known about individual fetal liver niches that support HSPC expansion, the 3-D constructs provide a model system in which to dissect the role of its individual cellular and matrix components in supporting CB maintenance, expansion, and differentiation. The results showed that, irrespective of the microenvironment used, the 3D-ECM structures led to the maintenance of a more primitive subpopulation of HSPC. In addition, it was shown that the timing and extent of expansion depended upon the biological component used, with HpB promoting the expansion of functional immature multipotent hematopoietic progenitor cells, and LvSt providing the optimal balance between preservation of primitive CB HSPC and expansion/differentiation.

### INTRODUCTION

Despite the advances made in *ex vivo* expansion of cord blood-derived hematopoietic stem and progenitor cells (CB-HSPC), challenges still remain regarding the ability to obtain, from a single unit, sufficient numbers of both long- and short-term repopulating cells, capable of functional

engraftment, to enable the treatment of an adolescent or adult patient [1–3].

We have previously shown that we can effectively expand CB-HSPC and drive the differentiation of these cells toward both the myeloid and lymphoid lineages in a serum-free culture system, using a feeder layer of adult human bone marrow (BM)-derived stromal cells [4–7]. Using this

system, we have optimized initial progenitor content and cytokine concentrations [7–9], and demonstrated that the expanded cells had the ability to engraft pre-immune animals [5]. Although the number of long-term engrafting hematopoietic stem cells (HSC) amplified in this culture system, due to the overall increase in cell numbers, the absolute percentage growth of these most primitive stem cells decreased with time in culture.

Recently, we developed three-dimensional (3D), liver extracellular matrix (ECM)-derived scaffolds [10, 11], that, when seeded with human fetal liver cells, create a hepatic-like tissue *in vitro*, in which hepatoblasts (HpB) and endothelial cells engraft in their putative native locations, and display typical endothelial, hepatic, and biliary epithelial markers [12, 13]. In these unique constructs, human fetal liver progenitor cells self-assemble inside the ECM-derived scaffolds to form 3D liver organoids that recapitulate several aspects of the hepato-biliary ontogeny [14], allowing us to investigate the effects of these surrogate fetal liver environments on CB-HSPC.

It is well known that, during development, the fetal liver is the main site of HSC expansion and differentiation [15]. Within the fetal liver, HSC actively cycle, and these cells outcompete adult HSC upon transplantation [15, 16]. Thus, hepatic tissue contains cellular niches that lead to true expansion, or, at the least, maintenance of primitive HSC [17, 18]. Although CB-HSPC possess intrinsic properties that confer greater proliferation capacity and clonogenic potential [19, 20], the initial divisional behavior of CB-HSPC is also dependent upon the environment [21]. For example, the stromal cell line AFT024 and fetal HpB, both of murine origin, have been shown, in two-dimensional (2D) cultures, to effectively preserve the self-renewal capacity of human and mouse HSC, respectively [21, 22]. In addition, endothelial cells [23, 24] and stromal cells/pericytes associated with portal vessels have recently been shown to play an important role in promoting CB expansion and fetal hematopoiesis, respectively [3].

Here, we developed an “*in vitro*” approach to investigate the effect of different 3D microenvironments on a primitive subpopulation of human CB-derived CD34<sup>+</sup> CD38<sup>−</sup> hematopoietic progenitor cells [25]. To this end, we seeded HpB or stromal cells/pericytes, both derived from fetal liver, in a natural 3D ECM to create distinct hepatic-like fetal niche constructs. Moreover, to determine whether liver-derived cells were essential to the generation of the 3D microenvironments, we also seeded adult BM-derived stromal cells/pericytes in the same 3D matrix as a control. These functionally integrated 3D milieus were then compared with their 2D culture counterparts. We showed that, overall, 3D microenvironments were better able to support the absolute percentage growth of CD34<sup>+</sup> CD38<sup>−</sup> cells in culture, and earlier CD33<sup>+</sup> myeloid progenitors.

## MATERIALS AND METHODS

### Three-Dimensional ECM-Derived Scaffolds (3D-ECM) Disks

Four to five week-old ferret livers (Marshall Bioresources, North Rose, NY) were decellularized as previously described in detail [26], separated into lobes, embedded in plastic molds using optimum cutting temperature (OCT) formulation of water-soluble glycols and resins (Sakura Finetek, Torrance, CA), and flash frozen with liquid nitrogen. Cryopreserved decellularized liver lobes were mounted onto a Leica CM1950 cryotome (Leica Biosystems,

Buffalo Grove, IL) set at  $-8^{\circ}\text{C}$  to  $-10^{\circ}\text{C}$ , in order to maintain the liver lobes at warmer temperatures, thereby facilitating thick and intact sectioning of liver lobes at 300  $\mu\text{m}$  thickness. To generate scaffold disks from liver sections, an 8-mm diameter biopsy punch, equipped with a plunger (Medline Industries, Mundelein, IL) was used. The disks were placed in a 48 well plate, and air-dried for up to 4–6 hours, after which they were washed carefully with multiple washes of phosphate-buffered saline (PBS), and stored in PBS at  $4^{\circ}\text{C}$  until ready for sterilization by gamma irradiation at a dose of 15Gy (J.L. Shepherd and Associates, Inc., San Fernando, CA). These scaffolds are comprised of highly conserved proteins and heavily cross-linked extracellular matrix (ECM) components like collagens, elastin, fibronectin, laminin, and proteoglycans, which retain the characteristic 3D architecture of the native liver [10, 11]. Human fetal HpB and stromal cells can repopulate these scaffolds, engrafting in their putative native locations, and displaying typical hepatic and biliary epithelial markers. These repopulated constructs express markers characteristic of the human fetal liver, such as albumin and  $\alpha$ -fetoprotein, they secrete urea, and they metabolize drugs, proving this approach can create functional, bio-engineered liver tissue *in vitro* [12, 13].

### Isolation and Culture of Human Fetal Liver Stromal Cells and HpB

Human fetal livers, between 18 and 20 weeks of gestation, were obtained commercially from Advanced Biological Resources (ABR, Alameda, CA). Detailed methods for the isolation of HpB have previously been described [26]. Briefly, liver tissue was enzymatically digested at  $37^{\circ}\text{C}$  using collagenase type IV (Worthington Biochemical Corporation, Lake Wood, NJ) and deoxyribonuclease (Roche Life Sciences, Mannheim, Germany). Following digestion, nonparenchymal cells were separated from the parenchymal cell fraction by density gradient centrifugation using Histopaque-1077 (Sigma-Aldrich, St. Louis, MO). HpB (present in the lower fraction) were re-suspended in Kubota's hepatoblast growth medium (KM) (PhoenixSongs Biologicals, Branford, CT), and plated on Collagen-IV ( $5\ \mu\text{g}/\text{cm}^2$ ) (Sigma-Aldrich, St. Louis, MO) and Laminin ( $1\ \mu\text{g}/\text{cm}^2$ ) (BD Biosciences, Sparks, MD) coated 15-cm culture plates and incubated at  $37^{\circ}\text{C}$  as previously described [10]. The upper fraction containing fetal liver stromal cells (LvSt) was plated in gelatin-coated tissue culture flasks in mesenchymal stem cell growth media (MSCGM) (Lonza, Walkersville, MD). Culture plates containing the different cell fractions were washed on the next day to remove nonadherent cells, and were then maintained in KM (HpB) or MSCGM (LvSt), respectively, for up to 7 days. The cells were cultured and expanded, and flow cytometric analysis demonstrated that LvSt displayed markers characteristic of a perivascular mesenchymal cell/pericyte population that we and others have identified in several different organs [27], including CD146, CD105, CXCL12, CD90, and CD44.

### Isolation and Culture of Adult BM-Derived Stromal Progenitor Cells/Pericytes

Heparinized human BM was obtained from healthy donors after informed consent according to guidelines from the Office of Human Research Protection at Wake Forest University Health Sciences. Low-density BM mononuclear cells (BMNC) were separated by Ficoll density gradient ( $1.077\ \text{g}/\text{ml}$  Sigma-Aldrich, St. Louis, MO) centrifugation and washed twice in Iscove's modified Dulbecco's medium (Invitrogen, Carlsbad, CA). BMNC were first enriched for the Stro-1<sup>+</sup> fraction using a Stro-1 antibody (R&D Systems,

Minneapolis, MN) and magnetic bead cell sorting (Miltenyi Biotec, Inc., Auburn, CA). Stro-1<sup>+</sup> cells were expanded in vitro at 37°C in 5% CO<sub>2</sub> humidified air, in MSCGM, using Fibronectin-coated tissue culture flasks. At a confluence of 60%–75%, cells were detached with 0.25% trypsin (Invitrogen Corp., Carlsbad, CA) for 3–5 minutes at 37°C. Trypsin was neutralized with media containing 10% fetal bovine serum (Thermo Fisher Scientific, Grand Island, NY), and cells were passaged at a 1:3 ratio into gelatin-coated tissue culture flasks in MSCGM. Characterization by flow cytometry, and by functional studies, demonstrated that these cells displayed markers characteristic of BM-derived mesenchymal cells/pericytes, including CD105, CD146, CXCL12, CD90, CD44, and CD29, and that they were able to undergo trilineage differentiation into adipocytes, cartilage, and bone [28].

### Culture of HpB, LvSt, and Bone Marrow-Derived Stromal Progenitor Cells on 3D-ECM Disks and on Tissue Culture Plates (2D)

Bone marrow-derived stromal progenitor cells (BMSPC) and LvSt were detached from culture plates using Trypsin-EDTA (Sigma-Aldrich, Grand Island, NY), while HpB were harvested using collagenase IV (Worthington Biochemical Corporation, Lake Wood, NJ). Sterilized 3D-ECM disks in 48-well plates were incubated with either MSCGM or KM for 30–45 minutes prior to cell seeding, and were then air-dried under sterile conditions. Cells were resuspended in the appropriate seeding medium and slowly pipetted onto the top of each disk, and incubated for about an hour at 37°C to allow cells to attach to the disks before adding appropriate culture medium. Identical numbers of BMSPC or LvSt ( $2 \pm 0.5 \times 10^5$ ) were seeded in 3D-ECM disks and in 2D gelatin-coated 48-well plates. HpB ( $2 \pm 0.9 \times 10^5$ ) were seeded onto collagen IV- and laminin-coated 48-well tissue culture plates. Three days after seeding, stromal cells in 3D and 2D cultures were inactivated by treatment with 25 µg/ml Mitomycin-C (Sigma-Aldrich, St. Louis, MO) for 30 minutes at 37°C. After inactivation, cells in 2D and 3D cultures were extensively washed with PBS to remove any residual Mitomycin-C.

### Isolation and Culture of CB CD34<sup>+</sup> Cells

Human CB samples were graciously provided by the NHLBI Biologic Specimen and Data Repository Information Coordinating Center. CB samples were thawed and CD34<sup>+</sup> cells isolated using magnetic cell sorting using the CD34 ultra-pure microbead kit (Miltenyi Biotec, Gladbach, Germany) following manufacturer's instructions. As determined by flow cytometric analysis, the percentage of CD34<sup>+</sup> cells after sorting varied little between the experiments ( $67.7\% \pm 5.4\%$ ). CD34<sup>+</sup>-enriched cells were then seeded in 48-well plates on top of 3D-ECM disks containing LvSt and HpB in KM (PhoenixSongs Biologicals, Branford, CT) or KM supplemented with 50nM of the GSK3i CHIR99021 (Tocris Biosciences, Bristol, U.K.) and 10 µM Thiazovivin (Tocris Biosciences, Bristol, U.K.) (KM + Drugs). CB-derived cells were also cultured in 48-well plates on top of confluent BM MSC, LvSt, or HpB, in 2D or 3D cultures, in QBSF-60 serum-free medium (Quality Biologicals, Inc., Gaithersburg, MD) supplemented with stem cell factor (SCF) (100 ng/ml), Fms-related tyrosine kinase 3 ligand (Flt-3L) (100 ng/ml), leukemia inhibitory factor (LIF) (10 U/ml), and basic fibroblast growth factor (bFGF) (5 ng/ml), at 37°C and 5% CO<sub>2</sub> humidified air for 12 days (SFM).

### Proliferative and Phenotypic Analysis of Ex Vivo Expanded Cells

Nonadherent hematopoietic cells were harvested every other day. Cell number was determined using a hemocytometer, and viability was determined by Trypan Blue exclusion (Gibco, Grand Island, NJ). Hematopoietic cells were stained according to manufacturer's instructions using the appropriate isotype controls and a panel of fluorescein isothiocyanate (FITC)-conjugated anti-CD38, CD33, and CD15; PE-conjugated anti-CD133, CD7, and CD14; and PerCP-conjugated anti-CD34, CD3, and CD45 antibodies (all from BD Biosciences, San Jose, CA) with the exception of the anti-CD133 antibody (Miltenyi Biotec, Gladbach, Germany). Stained cells were then run on a FACScaliber (BD, San Jose, CA), and the resultant data were analyzed using Cellquest software.

### Methylcellulose Colony Assays

Methylcellulose colony assays were performed by plating 10<sup>4</sup> cultured cells in 2 ml of MethoCult H4434 (Stem Cell technologies, Vancouver, BC, Canada) culture medium. To determine the clonogenic potential of each CB prior to culture, 10<sup>4</sup> freshly isolated CD34<sup>+</sup> cells were also plated in MethoCult H4434 and grown under identical conditions. The cultures were maintained at 37°C in a humidified atmosphere of 5% CO<sub>2</sub> in air, and hematopoietic colonies were identified and enumerated in situ at day 14 after seeding, with a Zeiss Axiovert 40C inverted microscope.

### Immunohistochemistry and Immunofluorescent Staining of Liver Organoids

Liver organoids cocultured with CB-derived CD34<sup>+</sup> cells were harvested every week, fixed overnight with 10% Neutral-Buffered Formalin (Sigma-Aldrich, Saint Louis, MO), and preserved in paraffin blocks using standard techniques. H&E staining was performed on 5-micron sections of the liver organoids after deparaffinization and rehydration as previously reported [10].

### Statistics and Data Analysis

Fold increase of total MNC was determined by dividing the number of total viable cells present at each specific day of analysis by the initial viable cell count. Fold increase of various lineage cells was calculated by multiplying the percentage of lineage-specific cells by the count of total viable cells present at each specific day of analysis, and dividing this number by the total number of lineage-specific cells prior to culture.

Experimental results are presented as the mean plus/minus the SEM, and were analyzed with Prism 6 (GraphPad Software, Inc., La Jolla, CA). Statistical significance of differences observed between the various experimental conditions were determined using two-way analysis of variance (ANOVA) followed by the Bonferonni-Šidák correction for multiple comparisons. A *p* value <.05 was considered to be statistically significant.

## RESULTS

### Defining Culture Strategies to Support Both Functionally Integrated 3D Microenvironments and Hematopoiesis

In order to maintain the viability of HpB seeded in 3D-ECM disks (HpB-3D-ECM), and simultaneously coculture CB-HSPC, we first determined the suitability of the culture media to be used. Three different media formulations were tested in parallel, to determine which was best able to both maintain HpB-3D-ECM and support

the growth of CB-HSPC: (a) HpB-specific Kubota medium, alone (KM) ( $n = 3$ ); (b) KM in combination with CHIR99021, a potent inhibitor of GSK3 and wingless-related integration site (WNT) activator, and Thiazovivin, a RHO/ROCK pathway inhibitor (KM + Drugs) ( $n = 3$ ), which was previously shown to support the differentiation of ES cells into HpB [29]; and (c) serum-free media ( $n = 3$ ) [30] containing the cytokines Flt-3L, SCF, bFGF, and LIF (SFM), which we had previously shown to promote the ex vivo expansion of CB-HSPC grown over 2D stromal layers [4].

Weekly evaluation of the total number of viable mononuclear cells present in the supernatant of the HpB 3D-ECM cultures using each of the different media formulations demonstrated that SFM was better able to support the growth of HSPC than KM or KM + Drugs (Fig. 1A), and that SFM was able to preserve HpB-3D-ECM constructs to the same extent as HpB-specific media (Fig. 1B). Since the dose of colony-forming units (CFU) is one of the most important parameters influencing CB engraftment [31], we evaluated the clonogenic potential of CB-HSPC in culture. Our data show that the growth was optimal under SFM conditions. Moreover, although the total number of mononuclear cells increased with time throughout the duration of culture (Fig. 1A), cells with both colony forming unit-granulocyte, erythrocyte, macrophage, megakaryocyte (CFU-GEMM) and colony forming unit granulocyte, macrophage (CFU-GM) potential were found to be present during the first week (Fig. 1C, 1D, respectively).

During fetal development, the liver is a hematopoietic organ [15, 16]; therefore, it was possible that the HpB used in these experiments contained trace amounts of residual hematopoietic cells, and could thus be providing additional numbers of HSPC to the cultures. Microscopic and supernatant evaluation of cultures of HpB-3D-ECM in the absence of CB-HSPC cultured in SFM, KM, or KM + Drugs, at regular intervals after seeding, demonstrated that cultures that had not been seeded with CB-HSPC were devoid of any hematopoietic cells. These results thus confirmed that there were no HSPC contaminants within the HpB preparations that could be contributing to the observed HSPC expansion (Fig. 1E). In addition, since the ECM can also play a role in cell and tissue behavior, by virtue of its ability both to arrange cells in a highly-ordered 3D array, and to serve as a reservoir of growth factors and cytokines [32–34], CB-HSPC were also cocultured under the same media conditions using “empty” acellular scaffolds ( $n = 3$ ). When grown under these conditions, the number and viability of CB-HSPC rapidly decreased, and no viable hematopoietic cells were obtained in these cultures, demonstrating that the cellular components, and not residual cues present within the 3D-ECM, were responsible for supporting CB-HSPC expansion (Fig. 1E). In addition, and in similarity to our previous findings [35], CB-HSPC grown in culture media alone did not proliferate and had decreased viability with the time in culture (data not shown).

#### **Influence of HpB-3D-ECM and HpB-2D Environments on Expansion of the More Primitive CB-HSPC**

Having determined that SFM was the best culture media to support HpB-3D-ECM, and established that the first week was the optimal time frame to expand CD34+ HSPC with enhanced clonogenic potential, we next determined if HpB-3D-ECM and HpB-2D cultures differed in their ability to support expansion of the more primitive CB-HSPC. The total number and the fold increase of CB-derived MNC during the first week in culture, with either HpB-3D-ECM ( $n = 3$ ) or HpB-2D ( $n = 3$ ) is shown in Figure 2A. As can be seen in this figure, total CB-derived MNC expansion was

similar between the two different culture systems, as assessed by live cell fold increase at day 2 and 4. However, at day 6, HpB-2D HSPC contained significantly higher numbers of MNC than their HpB-3D-ECM HSPC counterparts ( $p < .05$ ). The percentage of CD34+ cells in 2D and 3D cultures remained similar throughout the time in culture (Fig. 2B), with the percentage of CD34+ cells decreasing by 29.7% and 20.5% in HpB-2D and HpB-3D-ECM, respectively.

Despite these apparent similarities, however, differences between 2D and 3D environments became readily apparent when the more primitive fraction of HSPC were analyzed. During the first week in culture, percentages of CD34 + CD38– in HpB-3D-ECM cultures, as determined by flow cytometric analysis, were higher than in HpB-2D (day 2,  $p = .8$ ; day 6,  $p = .9$ ), and at day 4 of culture, this difference reached statistical significance ( $p < .05$ ) (Fig. 2C). In agreement with these results, the percentage of CFU-GEMM colonies/1,000 cells was significantly higher at day 4 in culture ( $p < .05$ ) (Fig. 2D) while no significant differences were seen in the percentage of CFU-GM colonies/1,000 cells. In addition, HpB-3D-ECM cultures favored expansion of CD33+ cells over other myeloid and lymphoid lineages (Supporting Information Table S1). Also of note is that, in HpB-3D-ECM HSPC cultures, the percentage of CFU-GEMM colonies/1,000 cells was significantly higher at day 2 and 4 of culture than it was in the initial cell population (Fig. 2D).

H&E staining performed on 3D-ECM disks at the end of the culture period confirmed that 3D-ECM was cellularized throughout the duration of the experiment (Fig. 2E).

#### **Comparison of the Ability of LvSt-3D-ECM and LvSt-2D Environments to Support CB-HSPC Populations**

It has been reported that fetal liver pericytes and stromal cell lines play an important role in promoting CB expansion and fetal hematopoiesis [3]. Therefore, we next investigated whether 3D environments prepared with human fetal liver stromal cells (LvSt-3D-ECM) could also support the expansion of CD34 + CD38– CB-derived cells. No significant difference was found between the LvSt-3D-ECM ( $n = 3$ ) and LvSt-2D culture system ( $n = 3$ ) regarding total CB-derived MNC expansion (Fig. 3A), or the percentage of CD34+ cells (Fig. 3B). In similarity to the HpB-based 3D microenvironment, LvSt-3D-ECM supported the more primitive fraction of HSPC. At day 2 and 4 of culture, the percentage of CD34 + CD38– cells in LvSt-3D-ECM HSPC cultures was significantly higher ( $p < .05$ ) than in their LvSt-2D counterparts (Fig. 3C). While the percentage of CFU-GEMM colonies/1,000 cells was significantly higher at day 4 in LvSt-3D-ECM HSPC cultures (Fig. 3D), on that same day the percentage of CFU-GM colonies/1,000 cells was significantly higher in the LvSt-2D HSPC cultures ( $p < .05$ ). Both LvSt-3D-ECM and LvSt-2D supported the differentiation of cells with myeloid and lymphoid phenotypes (Supporting Information Table S1). As with the HpB-3D-ECM cultures, H&E staining was performed on LvSt-3D-ECM disks at the end of the cultures to verify that 3D-ECM was present and cellularized throughout the duration of the experiment (Fig. 3E)

#### **Ability of BMSPC-3D-ECM and BMSPC-2D Environments to Support CB-HSPC Populations**

Since we had previously used BMSPC to successfully create 2D environments that expanded CB cells, we next investigated whether BMSPC were able to colonize 3D liver-derived extracellular matrix scaffolds, and to evaluate how HSPC cultured on these

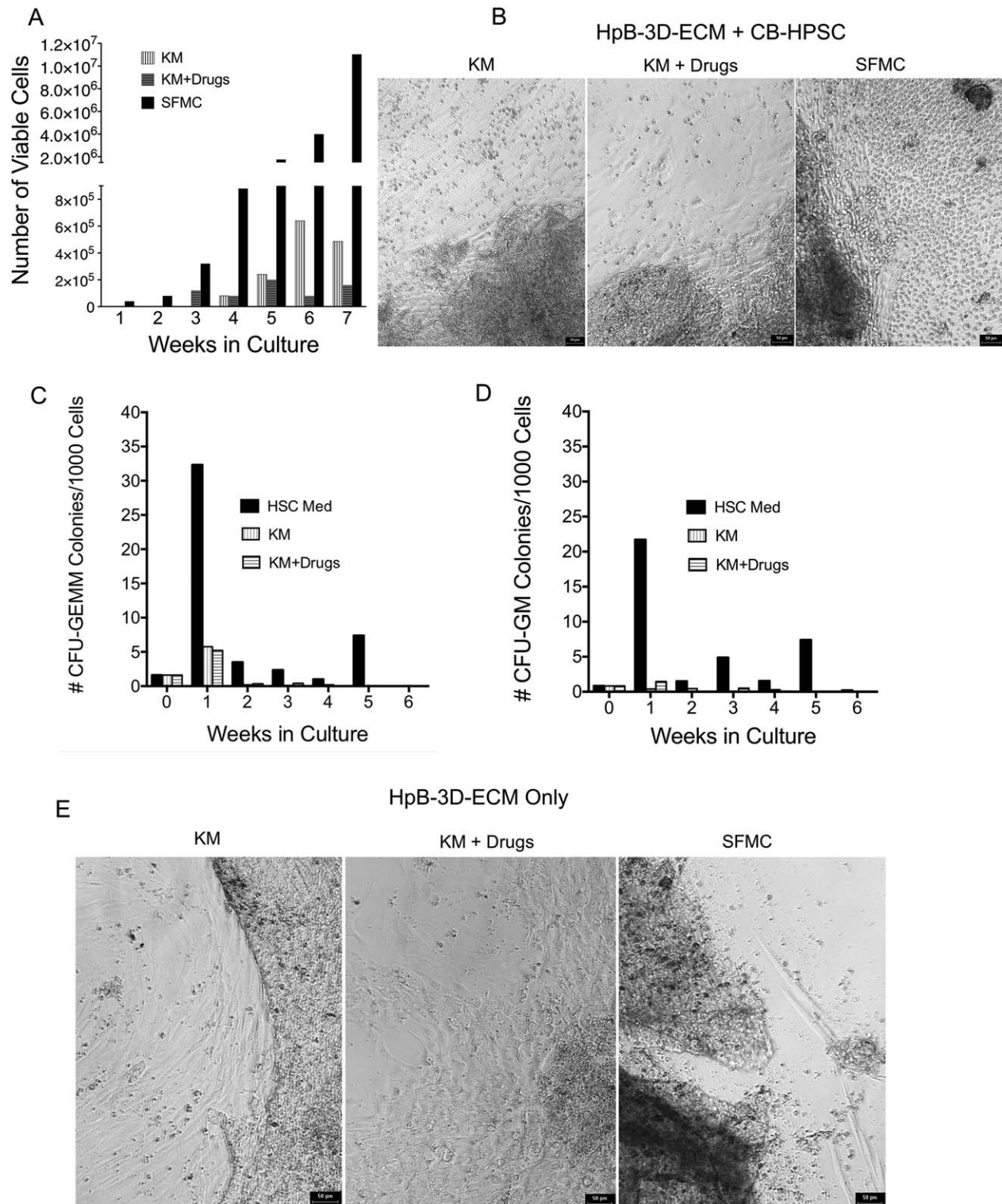


**Figure 1.** Defining culture strategies to support both functionally integrated 3D microenvironments and hematopoiesis. **(A):** Results from a representative experiment demonstrating the weekly evaluation of the total number of viable mononuclear cells in the supernatants of HpB 3D-ECM cultures using the various media formulations in a representative experiment. **(B):** Microscopic evaluation of viability of HpB-3D-ECM constructs with different media, demonstrating that KM, KM + Drugs, and SFM were all able to preserve HpB-3D-ECM constructs. **(C, D):** Results from the same representative experiment demonstrating clonogenic potential of CB-HSPC in culture; CFU-GEMM (C) and CFU-GM potential (D) was optimal under SFM conditions, and occurred during the first week. **(E):** Microscopic evaluation of cultures of HpB-3D-ECM, in the absence of CB-HSPC, using SFM, KM, or KM + Drugs, demonstrated that cultures that had not been seeded with CB-HSPC did not contain any hematopoietic cells. Transmitted light images were captured at  $\times 10$  with an Olympus IX-70 microscope. Abbreviations: 3D-ECM, three-dimensional liver-extracellular-matrix; CB-HSPC, cord blood-derived hematopoietic stem/progenitor cells; CFU-GEMM, colony forming unit-granulocyte, erythrocyte, macrophage, megakaryocyte; CFU-GM, colony forming unit granulocyte, macrophage; HpB, hepatoblasts; KM, Kubota's hepatoblast growth medium; SFMC, serum-free media+cytokines (Flt-3L, SCF, bFGF, and LIF).

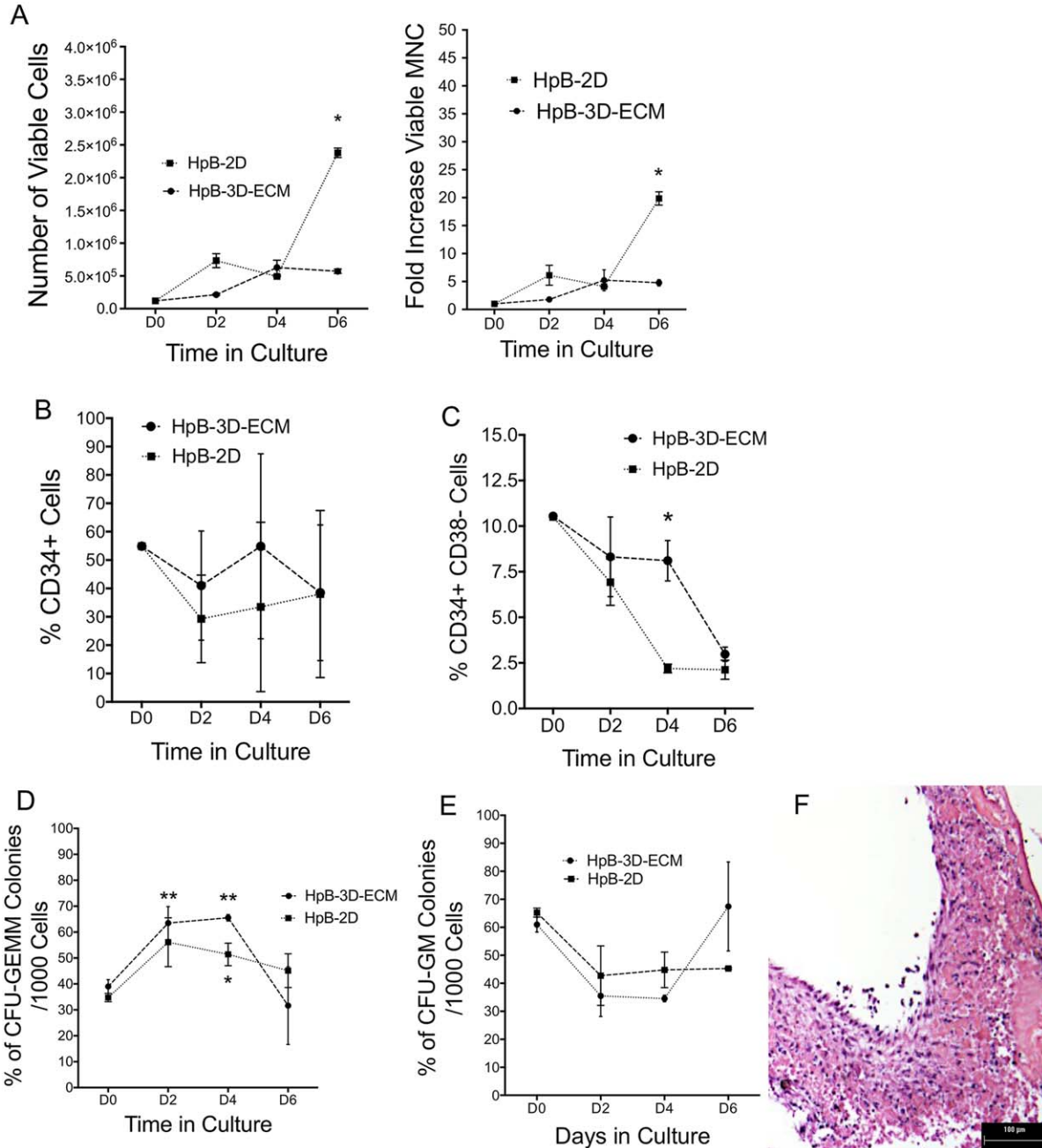


**Figure 2.** Influence of HpB-3D-ECM and HpB-2D environments on expansion of the more primitive CB-HSPC. **(A):** Cell and fold increase in total number of CB-derived MNC during the first week in culture; at day 6, HpB-2D HSPC contained significantly higher numbers of HSPC than their HpB-3D-ECM counterpart (\*,  $p < .05$ ). **(B):** Percentage of CD34+ cells in 2D and 3D cultures. **(C):** Daily percentages of CD34 + CD38- cells in HpB-3D-ECM cultures are higher than in HpB-2D (day 2,  $p = .8$ ; day 6,  $p = .9$ ; day 4 (\*,  $p < .05$ ). **(D):** Percentage of CFU-GEMM colonies/1,000 cells during the first week in culture; the percentage of CFU-GEMM colonies/1,000 cells was significantly higher at days 2 and 4 of culture than in the initial cell population (\*\*,  $p < .05$ ); comparison between 2D and 3D environments 3D environments showed had significantly higher percentage of CFU-GEMM colonies/1,000 cells at day 4 in culture than their 2D counterpart (\*,  $p < .05$ ). **(E):** Percentage of CFU-GM colonies/1,000 cells. **(F):** H&E staining performed on HpB-3D-ECM disks on the last day of cultures confirmed that HpB-3D-ECM was cellularized throughout the duration of the experiment. Abbreviations: 3D-ECM, three-dimensional liver-extracellular-matrix; CB-HSPC, cord blood-derived hematopoietic stem/progenitor cells; CFU-GEMM, colony forming unit-granulocyte, erythrocyte, macrophage, megakaryocyte; CFU-GM, colony forming unit-granulocyte, macrophage; HpB, hepatoblasts; MNC, mononuclear cells.

BMSPC-3D-ECM would compare to their 2D counterparts. The total number and the fold increase in CB-derived MNC during the first week in culture with BMSPC-3D-ECM ( $n = 3$ ) and BMSPC-2D ( $n = 3$ ) is shown in Figure 4A. As can be seen, the total CB-derived MNC expansion, as assessed by live cell fold increase, was similar between the two different cultures until day 4, but at day 6,

BMSPC-2D contained significantly higher total cell numbers than BMSPC-3D-ECM HSPC cultures ( $p < .05$ ). The percentage of CD34+ cells in 2D and 3D cultures remained similar throughout the time in culture, and was maintained from day 0 to day 6 (Fig. 4B). In similarity to what we had observed with the other 3D culture systems, BMSPC-3D-ECM maintained significantly higher

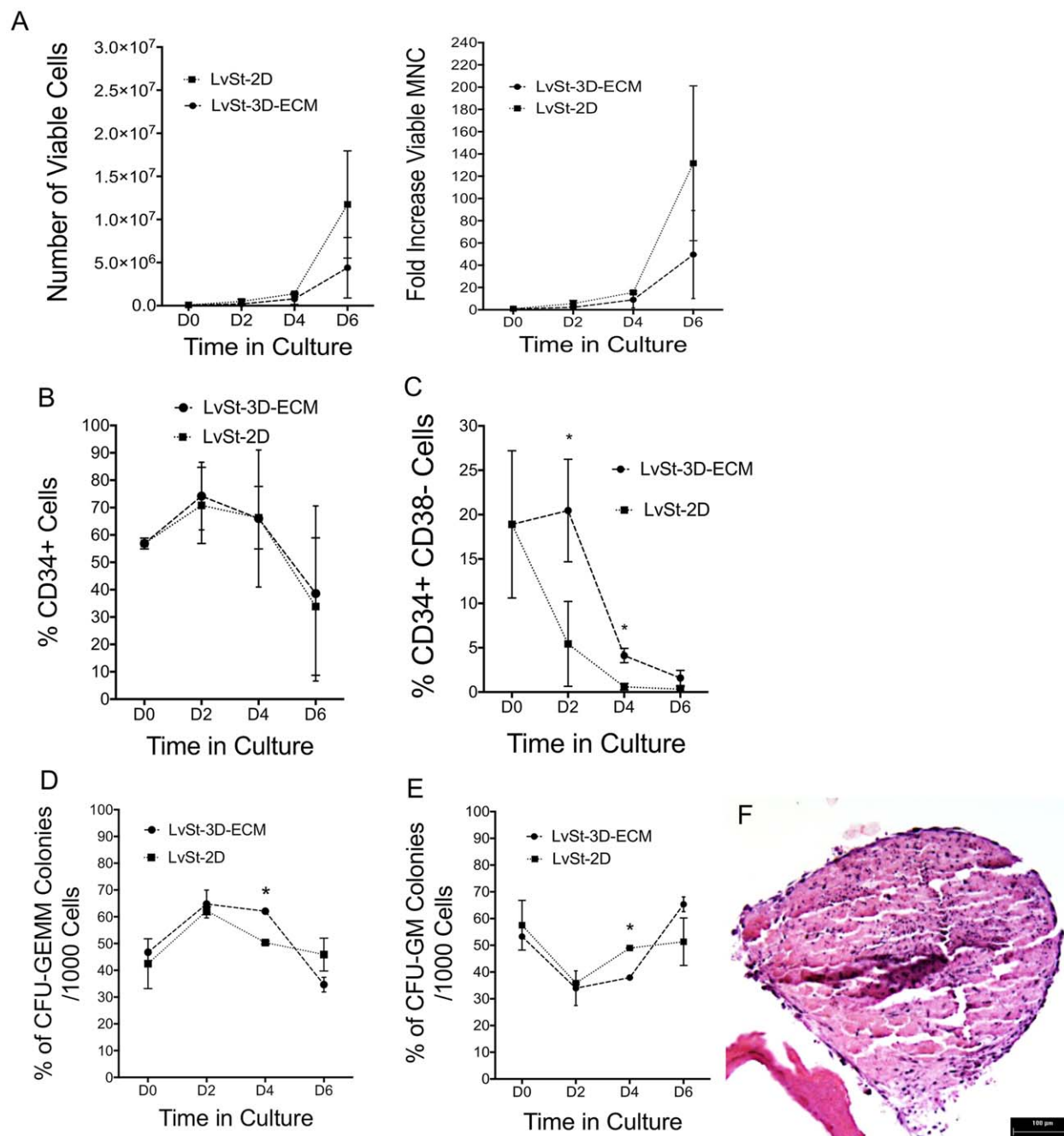


**Figure 3.** Comparison of the ability of LvSt-3D-ECM and LvSt-2D environments to support cord blood-derived hematopoietic stem/progenitor cells (CB-HSPC) populations. **(A):** Cell and fold increase in total number of CB-derived MNC during the first week in culture. No significant difference was observed between the LvSt-3D-ECM and LvSt-2D culture system, regarding total CB-derived MNC expansion. **(B):** Percentage of CD34+ cells in 2D and 3D cultures. **(C):** Daily percentages of CD34 + CD38- cells were significantly higher (\*,  $p < .05$ ) at days 2 and 4 of culture in LvSt-3D-ECM than in LvSt-2D. **(D):** Percentage of CFU-GEMM colonies/1,000 cells was significantly higher at day 4 in LvSt-3D-ECM HSPC cultures (\*,  $p < .05$ ) when compared to their 2D counterpart. **(E):** The percentage of CFU-GM colonies/1,000 cells was significantly higher (\*,  $p < .05$ ) at day 4 of culture in LvSt-2D compared to the LvSt-3D-ECM. **(F):** H&E staining on LvSt-3D-ECM disks at the conclusion of the cultures demonstrated that LvSt-3D-ECM was cellularized throughout the duration of the experiment. Abbreviations: 3D-ECM, three-dimensional liver-extracellular-matrix; CFU-GEMM, colony forming unit-granulocyte, erythrocyte, macrophage, megakaryocyte; CFU-GM, colony forming unit-granulocyte, macrophage; LvSt, fetal liver stromal cells; MNC, mononuclear cells.

percentages of CD34 + CD38- cells than 2D cultures (day 2,  $p < .05$ ; day 4,  $p < .05$ ) (Fig. 4C). However, in these BMSPC-based cultures, the percentages of CFU-GEMM and CFU-GM colonies/1,000 cells were similar in 2D and 3D conditions Figure 4D and 4E, respectively. In addition, as we had observed with the HpB-3D-

ECM, the BMSPC-3D-ECM also favored increase of CD33+ cells over other myeloid and lymphoid lineages (Supporting Information Table S1). As in the prior experiments, H&E staining confirmed that the BMSPC-3D-ECM disks were cellularized throughout the duration of culture (Fig. 4E).

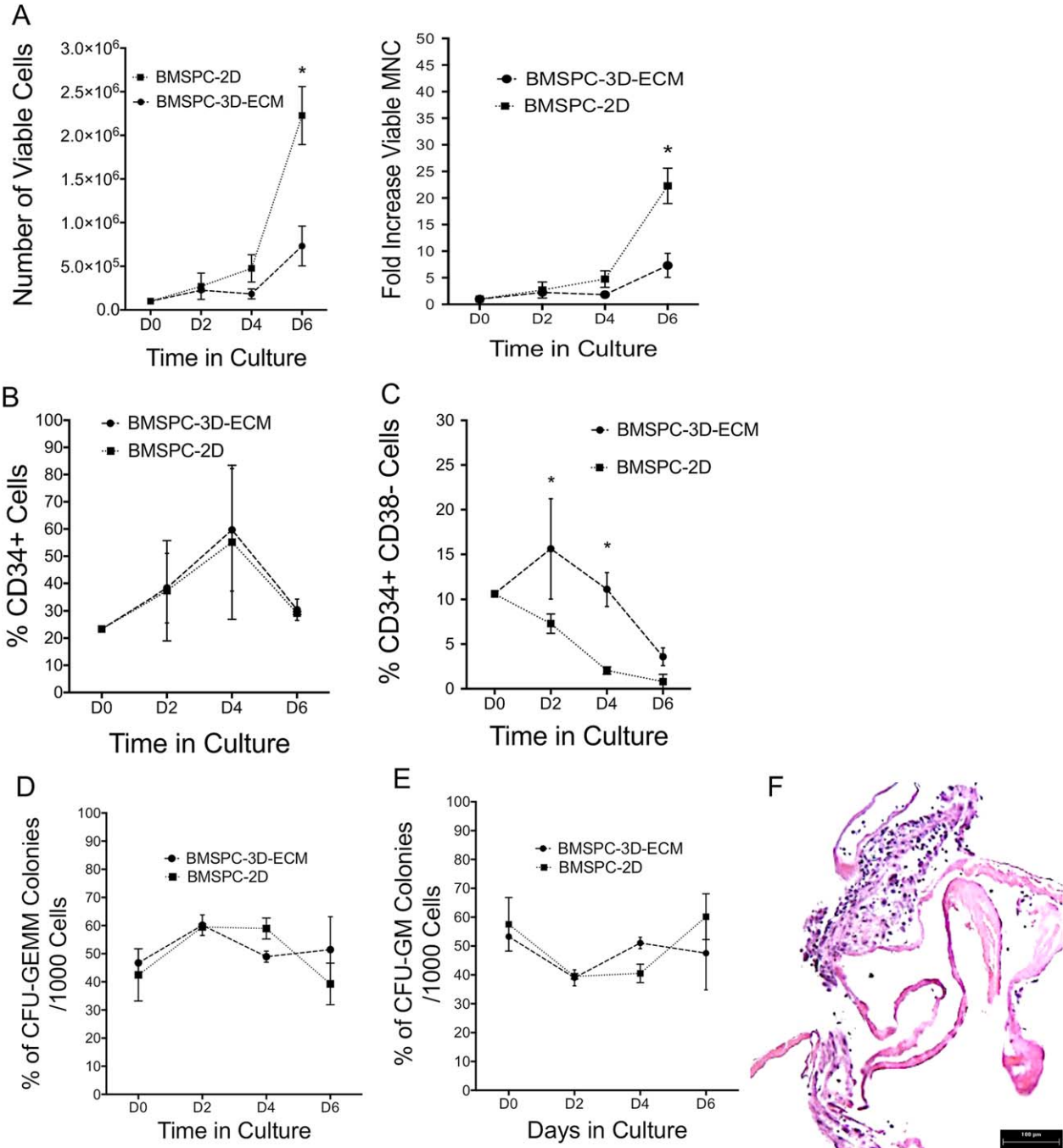


**Figure 4.** Ability of BMSPC-3D-ECM and BMSPC-2D environments to support cord blood-derived hematopoietic stem/progenitor cells (CB-HSPC) populations. **(A):** Cell and fold increase in total number of CB-derived MNC during the first week in culture; at day 6, BMSPC-2D contained significantly higher numbers of HSPC than their BMSPC-3D-ECM counterpart (\*,  $p < .05$ ). **(B):** Percentage of CD34+ cells in 2D and 3D cultures. **(C):** BMSPC-3D-ECM contained significantly higher percentages of CD34 + CD38- cells than 2D cultures (day 2, \*,  $p < .05$ ; day 4, \*,  $p < .05$ ). **(D):** Percentage of CFU-GEMM colonies/1,000 cells. **(E):** Percentage of CFU-GM colonies/1,000 cells. **(F):** H&E staining on BMSPC-3D-ECM disks at the conclusion of the cultures demonstrated that BMSPC-3D-ECM was cellularized throughout the duration of the experiment. Abbreviations: 3D-ECM, three-dimensional liver-extracellular-matrix; BMSPC, bone marrow-derived stromal progenitor cells; CFU-GEMM, colony forming unit-granulocyte, erythrocyte, macrophage, megakaryocyte; CFU-GM, colony forming unit-granulocyte, macrophage; MNC, mononuclear cells.

#### Comparison of the Influence of HpB-3D-ECM, LvSt-3D-ECM, and BMSPC-3D-ECM on CB-HSPC

Having determined that a 3D-ECM environment, regardless of the cell type, favored the maintenance of HSC with a more primitive phenotype, we next compared the impact of the different cell

types used to create the 3D-ECM environments, on expansion and differentiation of CB-HSPC.

The fold increase in total number of CB-derived MNC during the first 2 weeks in culture with HpB-3D-ECM ( $n = 3$ ), LvSt-3D-ECM ( $n = 3$ ), and BMSPC-3D-ECM ( $n = 3$ ) is shown in



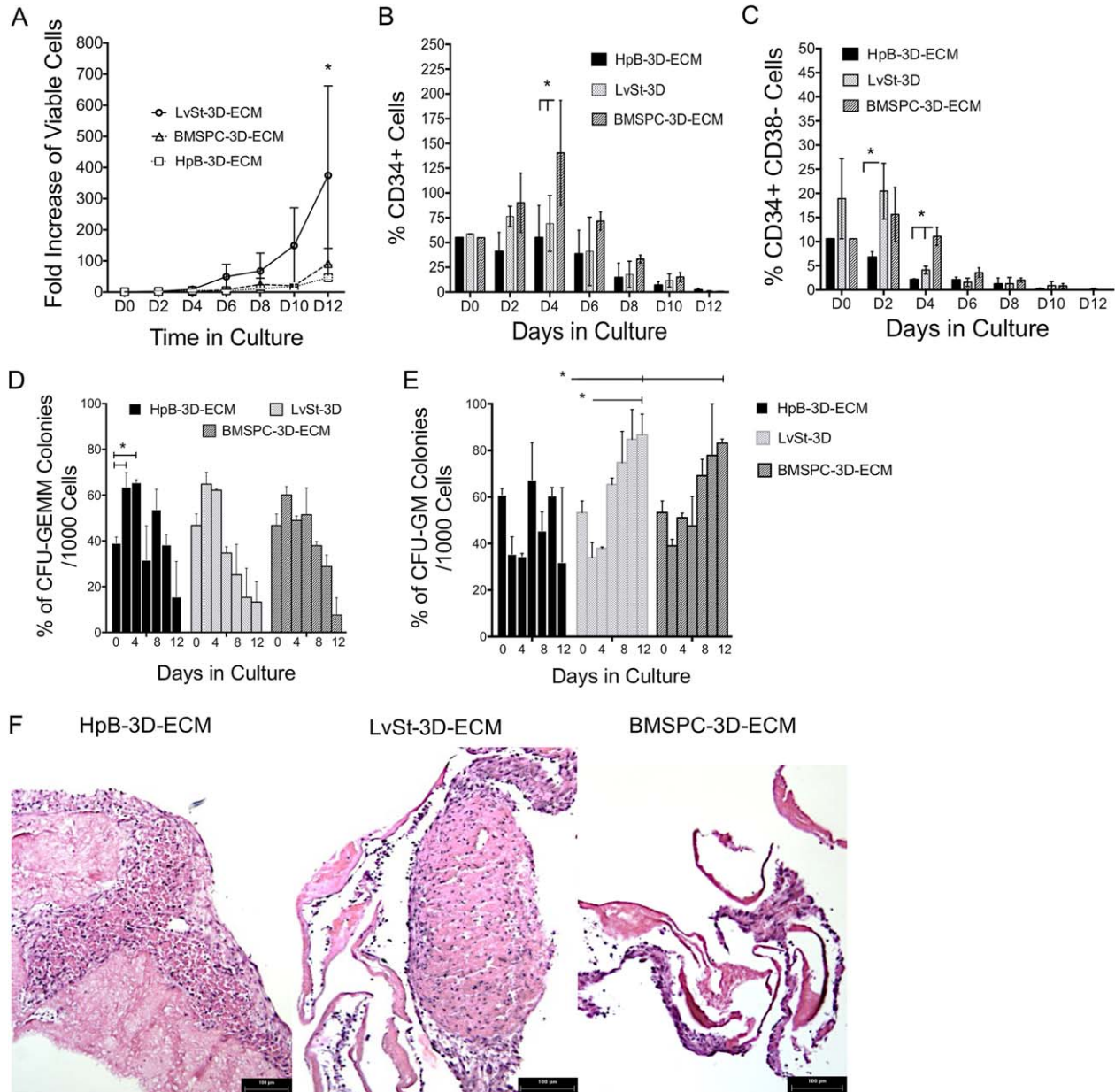


**Figure 5.** Comparison of the influence of HpB-3D-ECM, LvSt-3D-ECM, and BMSPC-3D-ECM on cord blood-derived hematopoietic stem/progenitor cells (CB-HSPC). **(A):** Fold increase in total number of CB-derived mononuclear cells (MNC) was similar between the different cultures systems during the first 6 days of culture, but extension of this evaluation to the second week of culture demonstrated that, at day 12, LvSt-3D-ECM contained significantly higher numbers of MNC than BMSPC-3D-ECM or HpB-3D-ECM (\*,  $p < .05$ ). **(B):** The percentage of CD34+ cells was significantly higher in BMSPC-3D-ECM (\*,  $p < .05$ ) at day 4 of culture when compared to LvSt-3D-ECM or HpB-3D-ECM, and at day 12, all cultures still contained CD34+ cells. **(C):** The percentage of CD34 + CD38- cells at day 2 was higher in LvSt-3D-ECM cultures when compared to HpB-3D-ECM (\*,  $p < .05$ ); At day 4, BMSPC-3D-ECM cultures contained significantly higher numbers of CD34 + CD38- cells than those with either BMSPC-3D-ECM or HpB-3D-ECM (\*,  $p < .05$ ); At day 12, only LvSt-3D-ECM cultures and HpB-3D-ECM contained CD34 + CD38- cells. **(D):** The percentage of CFU-GEMM/1,000 cells was similar for all 3D-ECM cultures, but only in LvSt-3D-ECM were the percentages of CFU-GM/1,000 cells on days 2 and 4 significantly higher than they had been on day 0 (\*,  $p < .05$ ). **(E):** The percentage of CFU-GM/1,000 cells, at day 12, was higher in LvSt-3D-ECM and BMSPC-3D-ECM when compared to HpB-3D-ECM on the same day. **(F):** Visualization of the different 3D-ECMs demonstrated that, at day 12, all of the constructs were still populated with cells. Abbreviations: 3D-ECM, three-dimensional liver-extracellular-matrix; BMSPC, bone marrow-derived stromal progenitor cells; CFU-GEMM, colony forming unit-granulocyte, erythrocyte, macrophage, megakaryocyte; CFU-GM, colony forming unit-granulocyte, macrophage; HpB, hepatoblasts; LvSt, fetal liver stromal cells.

Figure 5A. During the first 6 days of culture, the total CB-derived MNC expansion, as assessed by live cell fold increase, was similar between the different cultures systems. However, extension of this evaluation to the second week of culture

demonstrated that, at day 12, LvSt-3D-ECM contained significantly higher numbers of MNC than BMSPC-3D-ECM or HpB-3D-ECM ( $p < .05$ ). The percentage of CD34+ cells was significantly higher in BMSPC-3D-ECM ( $p < .05$ ) at day 4 of culture

when compared to LvSt-3D-ECM and HpB-3D-ECM, and at day 12, all cultures still contained CD34+ cells (Fig. 5B). LvSt-3D-ECM cultures contained higher percentages of CD34 + CD38– cells at day 2, when compared to HpB-3D-ECM ( $p < .05$ ), and by day 4, BMSPC-3D-ECM cultures contained significantly higher numbers of CD34 + CD38– than those with LvSt-3D-ECM and HpB-3D-ECM (Fig. 5C). Of note is that, by day 12, only LvSt-3D-ECM cultures and HpB-3D-ECM contained CD34 + CD38– cells. The percentage of CFU-GEMM/1,000 cells was similar for all 3D-ECM cultures (Fig. 5D), but the percentage of CFU-GM/1,000 cells, at day 12, was higher in LvSt-3D-ECM and BMSPC-3D-ECM when compared to HpB-3D-ECM (Fig. 5E). However, only in LvSt-3D-ECM was the percentage of CFU-GM/1,000 cells significantly higher than at day 0 (Fig. 5E). The only significant differences seen when evaluating numbers of mature myeloid cells during the time in culture occurred on day 10, when LvSt-3D-ECM contained significantly more CD15+ cells than BMSPC-3D-ECM ( $p < .05$ ) or HpB-3D-ECM ( $p < .05$ ), and on day 12, when LvSt-3D-ECM contained significantly more CD33+ and CD14+ cells, than BMSPC-3D-ECM ( $p < .05$ ) or HpB-3D-ECM ( $p < .05$ ) (Supporting Information Table S2). To rule out the possibility that the differences observed at day 12 were simply due to loss of the microenvironmental niches, the respective 3D-ECMs were visualized microscopically, which confirmed that the constructs were still populated with cells at day 12 of culture (Fig. 5E).

## DISCUSSION

For the past 20 years, CB-HSPC have served as a reliable source of hematopoietic stem and progenitor cells to treat malignant and nonmalignant disorders [36]. The advantages of using CB as a source of transplantable HSPC include the increased likelihood of a patient finding a compatible donor, its lower risk of inducing graft-versus-host disease, its ready availability, and the reduced probability of transmitting viral infections [36]. Still, the relatively low number of HSPC per CB unit, and the delayed kinetics of engraftment have hindered the use of CB-HSPC in adolescents and adults. Since the first CB transplant was performed more than 20 years ago [37], new strategies have been developed in an effort to overcome this limitation. The first attempts at *ex vivo* expansion of CB-HSPC used growth factors alone, and led to inadequate outcomes. However, when patients were transplanted with HSPC that had been cocultured in the presence of supportive stromal layers, the time to neutrophil and platelet reconstitution was significantly shortened [38]. Other approaches to expand the numbers of transplantable HSPC within a unit of CB have included or involved activation of endogenous Notch receptors [39], nicotinamide analogs [40], aryl hydrocarbon receptor antagonists [41], copper chelators [1], histone deacetylase inhibitors [42], and engraftment enhancers such as PEG2 [43] and CXCR4 [44]. These newer approaches have all shown great potential for the *ex vivo* expansion of CB-HSPC or accelerating their engraftment. Still, expansion of the true hematopoietic stem cell pool has been limited [2, 4, 45, 46]. We [4–7] and others [38] have previously shown that CB-HSPC can be effectively expanded and driven to differentiate toward both the myeloid and lymphoid lineages in a serum-free culture system, using a feeder layer of adult human BM-derived stromal cells. Using

this system, we have optimized initial progenitor content and cytokine concentrations [7–9], and demonstrated that the expanded human CB-HSPC had the ability to engraft pre-immune fetal sheep [5]. While the relative number of long-term engrafting HSC increased in this culture system, still, the absolute percentage growth of these most primitive stem cells decreased with time.

The importance of the composition and architecture of the microenvironment in inducing cell division/differentiation or expansion of CB-HSPC has been demonstrated by the use of mixed feeder layers within the same 2D culture [47], acellular matrices [48], and 3D culture systems [49–52]. Nevertheless, the challenge of expanding long-term repopulating HSC from a single unit, in such a way that sufficient numbers of HSC will be obtained to engraft an adult, while simultaneously increasing progenitor populations that are able to shorten time to engraftment, has yet to be solved [1, 2].

In the present study, we used natural 3D liver ECM scaffolds to recreate microenvironments that are known, during fetal development, to promote the expansion of true long-term repopulating HSC. In these unique constructs, human fetal liver progenitor cells self-assemble inside the ECM-derived scaffolds to form 3D liver organoids that recapitulate several aspects of the hepato-biliary ontogeny [14]. Moreover, since controlled cellular alignment plays a role in the biology and function of a tissue, the 3D liver scaffolds repopulated with single liver-derived cells, or other cell types, also provide a model system in which to test the role of 3D architecture and ECM components in the balance between the preservation and the differentiation of primitive CB-HSPC. The results show that ECM alone was either unable to support the viability, or inhibited the growth, of HSPC in culture, demonstrating that the presence of cellular components within the scaffolds was necessary for HSPC support. Analysis of the effects of different cellular microenvironments on HSPC, showed that, during the first 5 days of culture, total HSPC numbers did not vary considerably between 2D and 3D cultures. However, at day 6, BMSPC-2D and HpB-2D cultures contained significantly higher numbers of HSPC than BMSPC-3D-ECM and HpB-3D-ECM, respectively. At this time point, LvSt-3D-ECM had significantly higher numbers of HSPC than other 3D cultures, but not when compared with LvSt-2D-ECM, suggesting that LvSt-derived cells themselves are better able to support HSPC.

Analysis of the absolute percentage growth of CD34+ cells during the time in culture demonstrated that the 3D architecture did not significantly impact this outcome, which is in agreement with what has been reported with other types of 3D culture systems [51, 52].

While *in vivo* studies will be necessary to confirm that 3D microenvironments do not alter the ability of cultured HSPC populations to engraft, we were able to show that all of the 3D-ECM platforms contained significantly higher percentages of CD34 + CD38– cells than their 2D counterparts, demonstrating that, irrespective of the microenvironment used, the 3D-ECM structure led to the maintenance of a more primitive subpopulation of HSPC. In addition, longer-term maintenance of CD34 + CD38– cells (12 days), and the significantly higher percentage of CFU-GEMM colony output in HpB-3D-ECM and LvSt-3D-ECM also demonstrated that the combination of 3D-ECM organization with liver-derived cells preserved the more primitive HSPC during the time in culture. Of note is that only in

HpB-3D-ECM cultures was the percentage of CFU-GEMM/1,000 cells significantly higher at day 2 and 4 than in the initial HSPC population, suggesting that HSPC-HpB-3D-ECM cultures not only maintained, but supported the increase in functional immature multipotent hematopoietic progenitor cells. Furthermore, short-term evaluation of HSPC differentiation showed that, overall, 3D microenvironments were more efficient at sustaining earlier myeloid progenitors; while extending the time in culture to 2 weeks revealed that LvSt-3D-ECM was the most efficient environment for promoting the production of CD33, CD14, and CD15 positive cells.

## CONCLUSION

This study shows that the integration of cellular components with cellular components derived from microenvironmental niches was necessary for maintenance of HSPC viability in culture. Irrespective of the microenvironments used, the 3D-ECM structures led to the maintenance of a more primitive subpopulation of HSPC, as determined by flow cytometry and colony forming assays. In addition, the timing and extent of expansion depends upon the cellular component used, with HpB, promoting the increase of, functional immature multipotent hematopoietic progenitor cells, and LvSt providing the optimal balance between preservation of primitive CB HSPC and cell differentiation.

## REFERENCES

- 1 Tung SS, Parmar S, Robinson SN et al. Ex vivo expansion of umbilical cord blood for transplantation. *Best Pract Res Clin Haematol* 2010;23:245–257.
- 2 Dahlberg A, Delaney C, Bernstein ID. Ex vivo expansion of human hematopoietic stem and progenitor cells. *Blood* 2011;117:6083–6090.
- 3 Khan JA, Mendelson A, Kunisaki Y et al. Fetal liver hematopoietic stem cell niches associate with portal vessels. *Science* 2016;351:176–180.
- 4 da Silva CL, Goncalves R, Crapnell KB et al. A human stromal-based serum-free culture system supports the ex vivo expansion/maintenance of bone marrow and cord blood hematopoietic stem/progenitor cells. *Exp Hematol* 2005;33:828–835.
- 5 Goncalves R, Lobato da Silva C, Cabral JM et al. Stro-1(+) human universal stromal feeder layer to expand/maintain human bone marrow hematopoietic stem/progenitor cells in a serum-free culture system. *Exp Hematol* 2006;34:1353–1359.
- 6 Frias AM, Porada CD, Crapnell KB et al. Generation of functional natural killer and dendritic cells in a human stromal-based serum-free culture system designed for cord blood expansion. *Exp Hematol* 2008;36:61–68.
- 7 da Silva CL, Goncalves R, Porada CD et al. Differences amid bone marrow and cord blood hematopoietic stem/progenitor cell division kinetics. *J Cell Physiol* 2009;220:102–111.
- 8 Andrade PZ, dos Santos F, Almeida-Porada G et al. Systematic delineation of optimal cytokine concentrations to expand hematopoietic stem/progenitor cells in co-culture

with mesenchymal stem cells. *Mol Biosyst* 2010;6:1207–1215.

9 Andrade PZ, da Silva CL, dos Santos F et al. Initial CD34+ cell-enrichment of cord blood determines hematopoietic stem/progenitor cell yield upon ex vivo expansion. *J Cell Biochem* 2011;112:1822–1831.

10 Baptista PM, Siddiqui MM, Lozier G et al. The use of whole organ decellularization for the generation of a vascularized liver organoid. *Hepatology* 2011;53:604–617.

11 Baptista PM, Orlando G, Mirmalek-Sani SH et al. Whole organ decellularization - a tool for bioscaffold fabrication and organ bioengineering. *Conf Proc IEEE Eng Med Biol Soc* 2009;2009:6526–6529.

12 Lang R, Stern MM, Smith L et al. Three-dimensional culture of hepatocytes on porcine liver tissue-derived extracellular matrix. *Biomaterials* 2011;32:7042–7052.

13 Baptista PM, Siddiqui MM, Lozier G et al. The use of whole organ decellularization for the generation of a vascularized liver organoid. *Hepatology* 2011;53:604–617.

14 Vyas D, Baptista PM, Brovold M et al. Self-assembled liver organoids recapitulate hepatobiliary organogenesis in vitro. *Hepatology* 2017 [Epub ahead of print].

15 Morrison SJ, Hemmati HD, Wandycz AM et al. The purification and characterization of fetal liver hematopoietic stem cells. *Proc Natl Acad Sci USA* 1995;92:10302–10306.

16 Harrison DE, Zhong RK, Jordan CT et al. Relative to adult marrow, fetal liver repopulates nearly five times more effectively long-term than short-term. *Exp Hematol* 1997;25:293–297.

17 Brummendorf TH, Dragowska W, Lansdorp PM. Asymmetric cell divisions in

hematopoietic stem cells. *Ann NY Acad Sci* 1999;872:265–272.

18 Mikkola HK, Orkin SH. The journey of developing hematopoietic stem cells. *Development* 2006;133:3733–3744.

19 Kim DK, Fujiki Y, Fukushima T et al. Comparison of hematopoietic activities of human bone marrow and umbilical cord blood CD34 positive and negative cells. *STEM CELLS* 1999;17:286–294.

20 Hills M, Lucke K, Chavez EA et al. Probing the mitotic history and developmental stage of hematopoietic cells using single telomere length analysis (STELA). *Blood* 2009;113:5765–5775.

21 Punzel M, Liu D, Zhang T et al. The symmetry of initial divisions of human hematopoietic progenitors is altered only by the cellular microenvironment. *Exp Hematol* 2003;31:339–347.

22 Chou S, Lodish HF. Fetal liver hepatic progenitors are supportive stromal cells for hematopoietic stem cells. *Proc Natl Acad Sci USA* 2010;107:7799–7804.

23 Butler JM, Gars EJ, James DJ et al. Development of a vascular niche platform for expansion of repopulating human cord blood stem and progenitor cells. *Blood* 2012;120:1344–1347.

24 Gori JL, Butler JM, Kunar B et al. Endothelial cells promote expansion of long-term engrafting marrow hematopoietic stem and progenitor cells in primates. *STEM CELLS TRANSLATIONAL MEDICINE* 2017;6:864.

25 Hao QL, Shah AJ, Thiemann FT et al. A functional comparison of CD34+ CD38- cells in cord blood and bone marrow. *Blood* 1995;86:3745–3753.

26 Baptista PM, Vyas D, Moran E et al. Human liver bioengineering using a whole

## ACKNOWLEDGMENTS

This study was supported by NIH R21HL117704, and NHLBI Biologic Specimen and Data Repository Information Coordinating Center.

## AUTHOR CONTRIBUTIONS

G.A.P.: conception and design, financial support, data analysis and interpretation, manuscript writing, final approval of the manuscript; P.M.B.: conception and design, collection or assembly of data, data analysis and interpretation; C.D.P.: conception and design; S.S.: conception and design, financial support, data analysis and interpretation, final approval of the manuscript; S.M.: collection or assembly of data, data analysis and interpretation, manuscript writing; D.A.V.: collection or assembly of data, data analysis and interpretation; C.J.F., E.M., M.B., and G.A.L.: collection or assembly of data; Z.L.: provision of study materials.

## DISCLOSURE OF POTENTIAL CONFLICTS OF INTEREST

S.M., C.J.F., E.M., M.B., G.A.L., Z.L., and C.D.P. have nothing to disclose. P.M.B., S.S., and G.A.P. hold a patent on “Bioengineered Liver Constructs & Methods Relating Thereto” PCT/US2014/016331. D.V. is an employee of Biorg, Inc.

liver decellularized bioscaffold. *Methods Mol Biol* 2013;1001:289–298.

**27** Sanada C, Kuo CJ, Colletti EJ et al. Mesenchymal stem cells contribute to endogenous FVIII:c production. *J Cell Physiol* 2013;228:1010–1016.

**28** Chamberlain J, Yamagami T, Colletti E et al. Efficient generation of human hepatocytes by the intrahepatic delivery of clonal human mesenchymal stem cells in fetal sheep. *Hepatology* 2007;46:1935–1945.

**29** Yamazoe T, Shiraki N, Toyoda M et al. A synthetic nanofibrillar matrix promotes in vitro hepatic differentiation of embryonic stem cells and induced pluripotent stem cells. *J Cell Sci* 2013;126:5391–5399.

**30** Almeida-Porada G, Brown RL, MacKintosh FR et al. Evaluation of serum-free culture conditions able to support the ex vivo expansion and engraftment of human hematopoietic stem cells in the human-to-sheep xenograft model. *J Hematother Stem Cell Res* 2000;9:683–693.

**31** Page KM, Zhang L, Mendizabal A et al. Total colony-forming units are a strong, independent predictor of neutrophil and platelet engraftment after unrelated umbilical cord blood transplantation: A single-center analysis of 435 cord blood transplants. *Biol Blood Marrow Transplant* 2011;17:1362–1374.

**32** Schmeichel KL, Weaver VM, Bissell MJ. Structural cues from the tissue microenvironment are essential determinants of the human mammary epithelial cell phenotype. *J Mammary Gland Biol Neoplasia* 1998;3:201–213.

**33** Zschenker O, Streichert T, Hehlhans S et al. Genome-wide gene expression analysis in cancer cells reveals 3D growth to affect ECM and processes associated with cell adhesion but not DNA repair. *PLoS One* 2012;7:e34279.

**34** Carson DD. Extracellular matrix: Forum introduction. *Reprod Biol Endocrinol* 2004;2:1.

**35** da Silva CL, Goncalves R, dos Santos F et al. Dynamic cell-cell interactions between cord blood haematopoietic progenitors and the cellular niche are essential for the expansion of CD34+, CD34+CD38- and early lymphoid CD7+ cells. *J Tissue Eng Regen Med* 2010;4:149–158.

**36** Broxmeyer HE. Enhancing engraftment of cord blood cells via insight into the biology of stem/progenitor cell function. *Ann NY Acad Sci* 2012;1266:151–160.

**37** Gluckman E, Broxmeyer HA, Auerbach AD et al. Hematopoietic reconstitution in a patient with Fanconi's anemia by means of umbilical-cord blood from an HLA-identical sibling. *N Engl J Med* 1989;321:1174–1178.

**38** de Lima M, McNiece I, Robinson SN et al. Cord-blood engraftment with ex vivo mesenchymal-cell coculture. *N Engl J Med* 2012;367:2305–2315.

**39** Delaney C, Heimfeld S, Brashem-Stein C et al. Notch-mediated expansion of human cord blood progenitor cells capable of rapid myeloid reconstitution. *Nat Med* 2010;16:232–236.

**40** Peled T, Shoham H, Aschengrau D et al. Nicotinamide, a SIRT1 inhibitor, inhibits differentiation and facilitates expansion of hematopoietic progenitor cells with enhanced bone marrow homing and engraftment. *Exp Hematol* 2012;40:342–355.

**41** Boitano AE, Wang J, Romeo R et al. Aryl hydrocarbon receptor antagonists promote the expansion of human hematopoietic stem cells. *Science* 2010;329:1345–1348.

**42** Chaurasia P, Gajzer DC, Schaniel C et al. Epigenetic reprogramming induces the expansion of cord blood stem cells. *J Clin Invest* 2014;124:2378–2395.

**43** Hoggatt J, Singh P, Sampath J et al. Prostaglandin E2 enhances hematopoietic stem cell homing, survival, and proliferation. *Blood* 2009;113:5444–5455.

**44** Campbell TB, Hangoc G, Liu Y et al. Inhibition of CD26 in human cord blood CD34+ cells enhances their engraftment of nonobese diabetic/severe combined immunodeficiency mice. *Stem Cells Dev* 2007;16:347–354.

**45** Broxmeyer HE. Insights into the biology of cord blood stem/progenitor cells. *Cell Prolif* 2011;44(suppl 1):55–59.

**46** McNiece I, Harrington J, Turney J et al. Ex vivo expansion of cord blood mononuclear cells on mesenchymal stem cells. *Cytotherapy* 2004;6:311–317.

**47** Choi YS, Lim DS, Lim SM et al. Effects of mixed feeder cells on the expansion of CD34 cells. *J Biosci Bioeng* 2012;113:389–394.

**48** Tiwari A, Tursky ML, Mushahary D et al. Ex vivo expansion of haematopoietic stem/progenitor cells from human umbilical cord blood on acellular scaffolds prepared from MS-5 stromal cell line. *J Tissue Eng Regen Med* 2013;7:871–883.

**49** Mortera-Blanco T, Mantalaris A, Bismarck A et al. Long-term cytokine-free expansion of cord blood mononuclear cells in three-dimensional scaffolds. *Biomaterials* 2011;32:9263–9270.

**50** Schmal O, Seifert J, Schaffer TE et al. Hematopoietic stem and progenitor cell expansion in contact with mesenchymal stromal cells in a hanging drop model uncovers disadvantages of 3D culture. *Stem Cells Int* 2016;2016:4148093.

**51** Futrega K, Atkinson K, Lott WB et al. Spheroid coculture of hematopoietic stem/progenitor cells and monolayer expanded mesenchymal stem/stromal cells in polydimethylsiloxane microwells modestly improves in vitro hematopoietic stem/progenitor cell expansion. *Tissue Eng Part C Methods* 2017;23:200–218.

**52** Ferreira MS, Jahnen-Dechent W, Labude N et al. Cord blood-hematopoietic stem cell expansion in 3D fibrin scaffolds with stromal support. *Biomaterials* 2012;33:6987–6997.



See [www.StemCellsTM.com](http://www.StemCellsTM.com) for supporting information available online.